AGU ADVANCING EARTH AND SPACE SCIENCES

Water Resources Research®

RESEARCH ARTICLE
10.1029/2025WR040624

Special Collection:
Integrating In Situ, Remote Sensing, And Physically Based Modeling Approaches to Understand Global Freshwater Ice Dynamics

Evaluating Winter Turbulent Heat Fluxes in a Hydrodynamic-Ice Model of the Great Lakes

Gabriella Lükő[1,2,3], Eric J. Anderson[3], Christopher Spence[4], John D. Lenters[5], Peter D. Blanken[6], Erin Nicholls[7], and Péter Torma[1,2]

[1]National Laboratory for Water Science and Water Security, Department of Hydraulic and Water Resources Engineering, Faculty of Civil Engineering, Budapest University of Technology and Economics, Budapest, Hungary, [2]Department of Hydraulic and Water Resources Engineering, Faculty of Civil Engineering, Budapest University of Technology and Economics, Budapest, Hungary, [3]Colorado School of Mines, Hydrologic Science and Engineering, Golden, CO, USA, [4]Environment and Climate Change, Saskatoon, SK, Canada, [5]University of Michigan Biological Station, Pellston, MI, USA, [6]University of Colorado, Boulder, CO, USA, [7]University of Calgary, Calgary, AB, Canada

Key Points:

- Operational hydrodynamic model of the Great Lakes demonstrates skill of simulating open-water turbulent heat fluxes in winter
- Winter eddy covariance data should be used cautiously due to extreme weather conditions at remote locations
- Ice thickness, concentration, and temperature influence lake ice fluxes, and modeled fluxes are less accurate during periods of high ice

Supporting Information:

Supporting Information may be found in the online version of this article.

Correspondence to:

G. Lükő,
luko.gabriella@emk.bme.hu

Citation:

Lükő, G., Anderson, E. J., Spence, C., Lenters, J. D., Blanken, P. D., Nicholls, E., & Torma, P. (2025). Evaluating Winter turbulent heat fluxes in a hydrodynamic-ice model of the Great Lakes. *Water Resources Research*, *61*, e2025WR040624. https://doi.org/10.1029/2025WR040624

Received 28 APR 2025
Accepted 3 NOV 2025

Author Contributions:

Conceptualization: Gabriella Lükő, Eric J. Anderson, John D. Lenters, Peter D. Blanken, Péter Torma
Data curation: Gabriella Lükő, John D. Lenters, Erin Nicholls

Abstract

Turbulent heat fluxes are affected by and influence the temperature dynamics and ice conditions of lakes. Significant efforts have been made to develop operational hydrodynamic and ice models for large lakes such as the North American Great Lakes. However, the behavior of surface fluxes in these lakes has previously focused on the ice-free season and has not yet been fully assessed during winter conditions in the presence of ice. Given the importance of navigation support and regional weather forecasting, we therefore analyze operational configurations of the Great Lakes for modeled fluxes to evaluate them for open water, ice-covered, and partial ice conditions. We compare the modeled fluxes with eddy covariance-based observed fluxes from the Great Lakes Evaporation Network. While observed latent heat fluxes have periods of high values both during ice-free and ice-covered periods, we find that elevated open water fluxes in early winter can be well modeled. However, the modeled fluxes during ice-covered periods appear less accurate, where the errors are likely related to the simulated ice thickness. Thin ice has many small cracks, resulting in large fluxes nearly as high as over open water; very thick ice can reduce the latent fluxes to near zero, according to observations. Overall, the algorithms used in existing operational models show promise in resolving winter lake fluxes; however, further improvement may require adaptations to underlying ice and hydrodynamic model formulations.

1. Introduction

Amongst the world's largest lakes, the North American Great Lakes, hereafter Great Lakes, hold 21% of the global surface freshwater supply. The ecosystem of lakes is strongly affected by global climate change and increasing anthropogenic impacts (Woolway, Sharma, & Smol, 2022). Lakes have been noted as the key sentinels of climate change worldwide (Williamson et al., 2009) and observed to be warming and losing ice in response (Anderson et al., 2024; O'Reilly et al., 2015; Sharma et al., 2019; Woolway, 2023; Woolway et al., 2021). These changes affect the lakes' physical processes, closely interacting with the atmosphere. The meteorological conditions above the lake, determine lake hydrodynamics, temperature, ice, mixing, and transport conditions. At the same time, the water or ice surface temperature influences the atmosphere through the turbulent heat fluxes at the air-water and air-ice interfaces. These sensible and latent (evaporative) heat fluxes play key roles in the lakes' energy balance, while latent heat is one of the most critical loss components in the water balance. These processes significantly impact hydrologic, weather, and climate conditions, which are important factors in lake management, commercial navigation, and hydropower generation (Fry et al., 2022; Gronewold et al., 2018).

Globally, lakes are losing ice due to climate change, and several open questions remain regarding lake ice conditions (Culpepper et al., 2025). Ice concentration and thickness are both declining, resulting in ice safety concerns (Woolway, Huang, et al., 2022). The Great Lakes also experience fewer days of ice cover than before (Anderson et al., 2024). The increasing winter air temperatures, and thus the lower lake-air temperature differences, result in lower open water turbulent heat fluxes and less intense cooling and ice formation. With the decline of ice concentration, more fractional ice and thinner ice can be expected. Due to the combination of these impacts, the open water turbulent heat fluxes and evaporation in winter months may increase during times with sufficient lake-air gradients. Consequently, the increased heat and moisture in the air over the lake can impact the regional weather, causing extreme lake-effect precipitation events (Fujisaki-Manome et al., 2020a, 2020b).

Formal analysis: Gabriella Lükő, Eric J. Anderson, John D. Lenters, Erin Nicholls
Funding acquisition: Gabriella Lükő, Eric J. Anderson
Investigation: Gabriella Lükő, Christopher Spence, John D. Lenters, Peter D. Blanken, Erin Nicholls, Péter Torma
Methodology: Gabriella Lükő, Eric J. Anderson
Resources: Gabriella Lükő, Eric J. Anderson
Software: Gabriella Lükő, Eric J. Anderson
Supervision: Eric J. Anderson, Péter Torma
Validation: Gabriella Lükő
Visualization: Gabriella Lükő, Eric J. Anderson
Writing – original draft: Gabriella Lükő, Péter Torma
Writing – review & editing: Eric J. Anderson, Christopher Spence, John D. Lenters, Peter D. Blanken

Over the past several decades, the National Oceanic and Atmospheric Administration (NOAA) has developed an operational forecasting model, the Great Lakes Operational Forecast System (GLOFS) to address a broad array of stakeholder needs (Anderson et al., 2018; Schwab & Bedford, 1994), with the most recent version consisting of a coupled hydrodynamic-ice model. The basis of GLOFS is the Finite Volume Community Ocean Model (FVCOM) (Chen et al., 2003) and the Los Alamos Sea Ice model (CICE) (Hunke et al., 2017), which have both been originally successfully adapted and calibrated for the Great Lakes (Anderson et al., 2018). The CICE model is also the basis for the prediction of operational Great Lakes by Environment and Climate Change Canada (ECCC; Durnford et al., 2018). The NOAA-GLOFS provides real-time currents, water temperatures, and ice conditions (ice concentration, thickness, and velocity), which have been evaluated against available observations (Anderson et al., 2018). In general, lake-averaged ice concentrations agree with satellite-derived products, but these models can struggle in freezing and melting periods and to reproduce accurate ice concentrations and lake thermal structure on local scales (Anderson et al., 2018; Cannon et al., 2024), which could be partly due to limitations of the employed flux algorithms.

The use of FVCOM or CICE in NOAA-GLOFS and ECCC, or other large lake studies, means that the prediction of lake conditions relies on oceanographic algorithms that are embedded within these models to estimate air-water and air-ice heat exchanges. Specifically, these models use the Coupled Ocean-Atmosphere Response Experiment (COARE) for open-water fluxes, the CICE model for the fluxes in the presence of ice, and they both use roughness lengths and bulk transfer coefficients for the calculations derived for the sea surface as a function of atmospheric stability conditions. Many studies have shown that these coefficients vary from lake to lake due to size, morphology, and climate (Guseva et al., 2023). Even though Earth's largest lakes, like the Great Lakes, embody many processes similar to the coastal ocean, COARE's suitability may be questionable, for example, due to different wave states in lakes compared to oceanic conditions (Lükő et al., 2022). In the Great Lakes, COARE has been validated against eddy covariance (EC) observations during ice-free periods, mainly in summer, fall, and mild winters (Charusombat et al., 2018). Yet, CICE fluxes have not yet been evaluated against measurements for the Great Lakes, nor for full or partial ice cover. Overall, modeled turbulent fluxes in the operational Great Lakes models have not been validated in the wintertime when the greatest wind speeds, temperature differences, and, thus, evaporation rates occur, and therefore our study serves as a significant gap in large lake prediction (Charusombat et al., 2018; Fujisaki-Manome et al., 2017; Lenters et al., 2013).

The EC technique is still the most accurate and direct method for turbulent flux observation at single locations, but it is not cost-effective and is prone to many possible error sources. The Great Lakes Evaporation Network (GLEN) (Blanken et al., 2011; Nicholls et al., 2024) has been operating several EC measurement stations year-round for almost two decades. GLEN has one or two stations for each lake, typically located offshore. The long-term GLEN flux data have been used in many applications in the past, for example, lake-wide water balance estimations (Gronewold et al., 2015) and lake-atmosphere interaction pertinent to numerical weather predictions (Blanken et al., 2011; Sharma et al., 2018). Even though point measurements may only represent local fluxes, temperature, and ice conditions, validating the Great Lakes' hydrodynamic-ice models with these measurements helps us to understand the physical processes, including their spatial variability across some of Earth's largest lakes.

In this study, we evaluate surface turbulent flux predictions for the Great Lakes for the wintertime using the three-dimensional hydrodynamic-ice model used in operational forecasting and compare these predictions to EC observations for 4 years. This analysis provides the first assessment of flux algorithms used for large lakes in the winter period under partial ice coverage. The resulting analysis can support the future development of the model for more accurate forecasts of hydrodynamics and ice conditions for the Great Lakes and Earth's large lakes as a whole.

2. Methods

2.1. Data

Two data sets, primarily based on satellite observations, were used in our analysis: The U.S. National Ice Center and Canadian National Ice Service Analysis (NIC) (Assel, 2005) and the Great Lakes Surface Environmental Analysis (GLSEA) (Schwab et al., 1999). NIC and GLSEA data consist of daily gridded charts of ice type, ice concentration (a_{ice}), ice thickness (v_{ice}), ice floe size estimation, and water surface temperatures (T_w) for the ice-free part of the lakes with 1.8×1.8 km spatial resolution. In the case of cloudy periods, data were gap-filled with

10.1029/2025WR040624

Figure 1. Great Lakes Evaporation Network sites (red dots) with photos of the stations used in the analysis, including Stannard Rock Lighthouse at Lake Superior, White Shoal Lighthouse at Lake Michigan, and Spectacle Reef Lighthouse at Lake Huron. Eddy-covariance and routine weather measurements are carried out at the top of these lighthouses (Blanken et al., 2011; Spence et al., 2011).

interpolation spatially and temporally. We note that there are no direct routine measurements of ice thickness in the Great Lakes. Instead, there are only ice thickness categories that provide a potential thickness range, which are inferred from ice-type observations and expert judgment. However, these estimates can still be useful for analyzing predicted fluxes. The GLEN has available turbulent flux data between 2008 and 2022 at several locations over the lakes (Blanken et al., 2011; Nicholls et al., 2024). We used data from Lake Superior's Stannard Rock Lighthouse (STD), Lake Michigan's White Shoal Lighthouse (WSL), and Lake Huron's Spectacle Reef Lighthouse (SRL) (Figure 1). Eddy-covariance data consisted of 30-min sensible (H) and latent heat fluxes (LE) with basic flux corrections, removal of spikes, and visual level of quality control (Spence et al., 2011). The measurement heights are 32 m at STD, 43 m at WSL, and 30 m at SRL stations above the mean water surface. Further details about the stations' instrumentation can be found in Nicholls et al. (2024). STD had two gas analyzers, the Licor KH20 krypton hygrometer and the Campbell Scientific LI-7500 IRGA, which were working simultaneously when available, but in the GLEN data, there was only one variable (which was a mix of available data). Unfortunately, in the simulated years, data from only one sensor was available at any given time. The other two stations, SRL and WSL, had single KH20 instruments. We note that there are other stations in the GLEN database that have not been used in this study due to data sparsity, quality issues, or the unique location of those stations, which are less likely to represent water or ice conditions of the Great Lakes as compared to the three stations chosen.

2.2. Hydrodynamic-Ice Model

The FVCOM three-dimensional hydrodynamic model (Chen et al., 2003) solves the Reynolds-averaged Navier-Stokes and transport equations and uses the Smagorinsky turbulence model horizontally and the Mellor-Yamada 2.5 model vertically. The model solves the equations on an unstructured triangular mesh. The model's horizontal resolution ranges from 50 m near coastlines to 2.5 km offshore (around 1.6, 1.8, and 2 km near SRL, WSL, and STD stations, respectively), and it has 21 evenly distributed sigma layers vertically for all lakes. We used NOAA-GLOFS's current version model settings (Anderson et al., 2018). The domain consists of a separate model for Lake Superior and a combined one for Lake Michigan-Huron.

The model's boundary conditions are the surface turbulent momentum and heat fluxes. For the open water heat fluxes, FVCOM uses the Coupled Ocean-Atmosphere Response Experiment (COARE) bulk parameterization (Fairall et al., 2003). COARE performs a few-step iteration to estimate the fluxes using the Monin-Obukhov similarity theory from routine meteorological input to take atmospheric stability conditions into account.

The Los Alamos Sea Ice Model's (CICE) unstructured grid version is two-way coupled with the FVCOM model to calculate ice growth, melt, and movement. The model includes ice dynamic processes, elastic-viscous-plastic rheology, ice thermodynamics, and a dynamic albedo that depends on ice thickness, snow depth, and surface temperature. The FVCOM version of CICE has been parameterized for freshwater lake conditions to improve the simulations of ice concentrations, and the modifications are part of the publicly available FVCOM code (v3.2 and

10.1029/2025WR040624

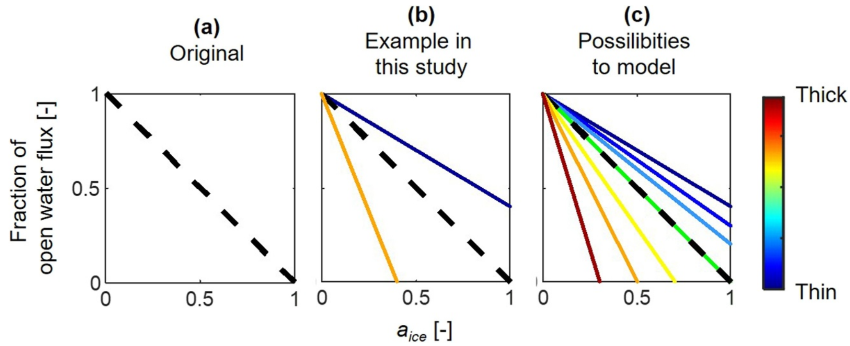

Figure 2. Fraction of open water flux as a function of ice concentration (a) in the Finite Volume Community Ocean Model model (b) in the modified calculations shown in this study as an example and (c) possible functions to test and model in the future.

after) and have been applied in several Great Lakes studies. The full extent of the freshwater parameterizations is available in the FVCOM source, and descriptions are detailed in recent literature (Fujisaki-Manome et al., 2020a, 2020b; Lin et al., 2022). Most notably, the freshwater modifications included changes to the ice thickness categories (5, 25, 65, 125, and 205 cm), use of Hibler's Law for ice strength, alternative ridging parameterization for freshwater ice, minimum thickness for frazil ice, and salinity-related adjustments. The fluxes in CICE are calculated using bulk transfer coefficients for both air-ice and ice-water interactions using a couple-step iteration considering atmospheric stability conditions.

We employed an interpolated meteorological forcing field according to the NOAA Great Lakes Coastal Forecast System method (Croley, 1989; Liu & Schwab, 1987; Phillips & Irbe, 1978; Resio & Vincent, 1977; Schwab & Bedford, 1994; Schwab & Morton, 1984), using all the available stations around the lakes including the GLEN station meteorology. The input data includes 10-m wind, shortwave and longwave radiation, 2-m air temperature, humidity, and pressure. The model's initial condition for the water temperature was set as the GLSEA observed temperature for the well-mixed surface mixing layer, and 4°C below.

We chose different medium-to high-ice years for the simulations when flux data were available. Four winter seasons were simulated from December 1st to May 1st: 2013–2014, 2014–2015, 2017–2018, and 2018–2019. Michigan WSL station did not have latent heat flux data for 2014–2015, and Superior STD station did not have any flux data for 2017–2018 and 2018–2019.

We evaluate the model simulations first by ice concentration (a_{ice}), ice thickness (v_{ice}), and water surface temperatures (T_w). Then, we analyze the turbulent sensible (H) and latent heat fluxes (LE). We compare these variables locally using data from the grid nearest to the stations. To evaluate each flux model, we separately look at the COARE fluxes for fully open water conditions and then the CICE-based turbulent fluxes for nearly 100% ice concentrations. We also check the fluxes during partial ice cover, such as both fluxes (F) are currently calculated according to the ratio of ice concentration:

$$F = F_{\text{CICE}} \cdot a_{\text{ice}} + F_{\text{COARE}} \cdot (1 - a_{\text{ice}}) \tag{1}$$

where F is the flux (either sensible or latent heat), F_{CICE} is the ice surface flux, F_{COARE} is the open water flux, and a_{ice} is the ice concentration.

This means that the model currently does not account for ice thickness in the flux fractioning, only the ice concentration (Figure 2a). We suggest that the open water flux fraction should be modified based on the ice thickness. Thin ice can have many cracks (not represented by the spatial resolution of either the FVCOM-CICE model or the NIC data), and also during melting, water on top of the ice could result in extra water fluxes. As an example, we show a simple modification (Figure 2b), where we modify the very thin ice ($v_{\text{ice}} < 100$ mm) and very thick ice ($v_{\text{ice}} > 500$ mm). Thin ice fluxes are increased by the higher open water flux ratios, and thick ice fluxes are reduced by less open water fluxes, only in the fractioning calculations. Future studies should apply other linear or non-linear functions for different ice thickness ranges in the FVCOM model to test the coupled effect of

Table 1
Finite Volume Community Ocean Model and National Ice Center Ice Concentration RMSEs for Each Lake Average and Station for Each Simulated Winter

	Huron		Michigan		Superior		All sites	
Ice concentration RMSE [–]	Lake avg.	SRL	Lake avg.	WSL	Lake avg.	STD	Lake avg.	Station
2013–2014	0.12	0.27	0.16	0.30	0.30	0.43	0.19	0.33
2014–2015	0.13	0.42	0.11	0.32	0.28	0.44	0.17	0.39
2017–2018	0.07	0.29	0.05	0.24	–	–	0.06	0.27
2018–2019	0.08	0.23	0.04	0.31	–	–	0.06	0.27
All winters	0.10	0.30	0.09	0.29	0.29	0.44	0.16	0.34

modified fluxes, temperatures, ice concentration, and thickness to improve the operational hydrodynamic-ice model forecasts in the Great Lakes (e.g., Figure 2c).

3. Results

3.1. Ice Conditions and Surface Temperatures

We start our model evaluation by examining the Root-Mean Square Error (RMSE) between simulated and observed ice concentrations. We looked at the model performance based on lake averages and locally at the stations (Table 1). For the analysis at the stations, we used the closest NIC grid and FVCOM node because the spatial variability was low near the stations; in contrast, the footprint of the flux towers might be smaller than the NIC and FVCOM grid resolution. All the ice concentration time series for each winter and station can be found in Figure S1 in Supporting Information S1. We found that lake averages were captured well with the model, while there is high variability of model performance at the station locations. As a representative example, Figures 3a and 3b show time series of modeled and observed ice concentrations for Lake Huron in winter 2014–2015. We see that the model only slightly overestimates the amount of ice concentration by considering the lake average. However, ice concentrations are highly overestimated at the Spectacle Reef station (SRL). FVCOM showed over 50% ice in January and March and did not capture the low ice concentration found in the NIC.

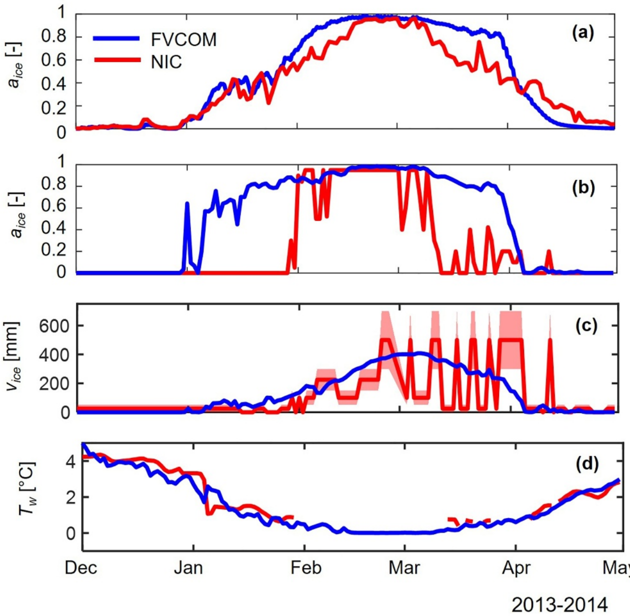

Figure 3. Time series of ice conditions for Lake Huron in winter 2014–2015, (a) lake average ice concentrations, (b) local ice concentrations, (c) local ice thickness, and (d) local water surface temperatures at Spectacle Reef station with Finite Volume Community Ocean Model model (blue) and National Ice Center and Great Lakes Surface Environmental Analysis data (red).

We calculated RMSEs between the modeled and observed ice data for each lake and station for each winter (Table 1). We found that the lake average RMSEs were much lower than locally at the stations, with RMSEs of 16% for lake average and 34% at the stations for all lakes and all winters. The deepest lake, Lake Superior, had the highest errors among the lakes, similar to previous studies (Anderson et al., 2018; Yeo et al., 2024). In 2017–2018 and 2018–2019, RMSE was smaller at Lake Michigan and Huron, but Lake Superior's errors are not included due to a lack of data and, thus, simulations. At the station locations, the modeled ice concentration errors vary from year to year and station to station, as the RMSEs show, between 23% and 44%. Generally, for deep water at the Stannard Rock station (STD), the RMSEs are high for both years. For the shallow water and thick ice at White Shoal station (WSL), the RMSEs are somewhat lower than at SRL, with more water and ice movement, where errors vary yearly.

Although there are no direct ice thickness observations, we attempt to compare modeled ice thickness with the NIC estimated minimum and maximum thickness ranges. For example, in Figure 3c, we show modeled ice thickness compared to the NIC estimates at Lake Huron's SRL station in the winter of 2014–2015. We see the same thickness overestimation of FVCOM as the concentrations, but the model cannot capture the transient ice movement around the site. NIC shows that thick and thin ice are passing by the station. For all winters and stations, the ice thickness comparisons can be

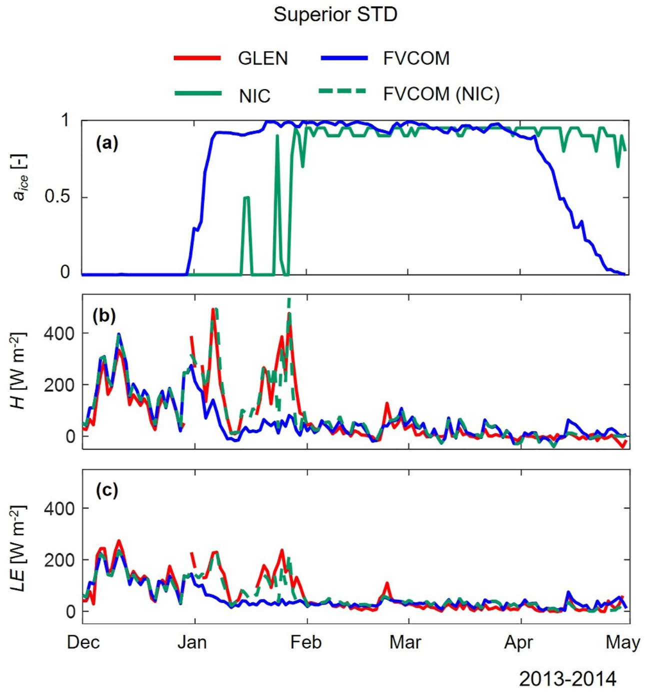

Figure 4. Time series of (a) ice concentration from the Finite Volume Community Ocean Model (FVCOM) and National Ice Center (NIC), (b) sensible and (c) latent heat fluxes with the FVCOM model, Great Lakes Evaporation Network data, and the NIC ice-fractioned FVCOM at Lake Superior's Stannard Rock station in winter 2013–2014.

found in Figure S2 in Supporting Information S1. The ice thickness at SRL was simulated well except for 2013–2014, with high model overestimation. In comparison, WSL has a higher thickness in general. In the first part of the winter, it is captured well by FVCOM, where the values are close to the bottom of the NIC thickness ranges; then, later in the winter, the model underestimates NIC values.

In regard to surface water temperature comparisons with the satellite-based GLSEA, the SRL station is taken as a representative example Figure 3 for the winter of 2014–2015 (Figure 3d). The model closely follows the daily GLSEA surface temperature. In these 5 months, the water surface temperature drops from 4 to nearly 0°C and freezes, then slowly increases to 3°C. Figure S3 in Supporting Information S1 shows all winter and station time series.

3.2. Turbulent Heat Fluxes

We analyzed the Great Lakes' turbulent heat fluxes locally. We compared simulated and observed sensible and latent heat fluxes at the three stations. In Figure 4, we show modeled and observed ice concentrations, as well as sensible and latent heat flux time series for STD station in winter 2013–2014. In this example, the error between modeled and observed fluxes is high, but the source of model error is in the simulated ice concentrations. In January 2014, both turbulent heat fluxes were highly underestimated by the model. At the same time, the model shows high ice cover, while the NIC shows mostly ice-free conditions until the end of January 2014. In April 2014, the model showed gradually melting ice with lower ice concentrations, while the NIC observation still showed high ice concentrations. The fluxes in the model during partial ice cover are calculated by fractioning by the ratio of the open water and ice fluxes based on ice concentrations (Equation 1). We recalculated the modeled fluxes using the NIC instead of the FVCOM ice concentrations to reduce the effect of ice errors in evaluating COARE and CICE fluxes. Figure 4 shows that the model flux errors are highly reduced, especially when there is more open water than the model assumes. As a result, only NIC ice-corrected fluxes are analyzed from this point. While the flux errors are significantly reduced when NIC is used for ice concentration correction, we note that this will partly introduce uncertainty associated with errors in the NIC ice data because its spatial resolution may be larger than the flux tower's footprint. Nevertheless, this shows that the estimates are reliable if the lake ice concentrations are adequately resolved, and thus, more generally, the CICE flux algorithm is able to provide reasonable estimates.

In Figure 5, we show the time series of ice with NIC and sensible and latent heat fluxes with the FVCOM model and the GLEN data at all stations for all winters. The NIC ice fractioning results in low deviations from observations for the sensible heat fluxes for all simulations. At the same time, we found high latent heat flux deviations in many cases but not at all times or locations. Generally, latent heat flux discrepancies are more frequent at the beginning and middle of winter and less so in the spring months. We found no significant difference in the atmospheric, hydrodynamic, or ice conditions between these periods; however, the combination of precipitation and low air temperatures may have led to the icing on the instrument, producing unrealistic flux calculations. We note that WSL, SRL, and STD all have KH20 krypton hygrometers, while STD additionally has an LI-7500 IRGA installed and running during most years. Only the KH20 was working in 2014–2015, while only the LI-7500 IRGA instrument was working in 2013–2014 at STD. Frank and Massman (2023) show that the different EC instruments may result in different flux errors, possibly due to limited calibration, which was not possible to carry out sufficiently in such remote locations at the lighthouses during winter. In the Discussion, we show long-term winter latent heat fluxes with both the KH20 and LI-7500 instruments at STD from the AmeriFlux database that support our previous findings about uncertain KH20 data. For this reason, in the following sections, uncertain values in the GLEN data are excluded and marked in light red colors in the flux time series. These GLEN data uncertainties are assessed in detail in the Discussion.

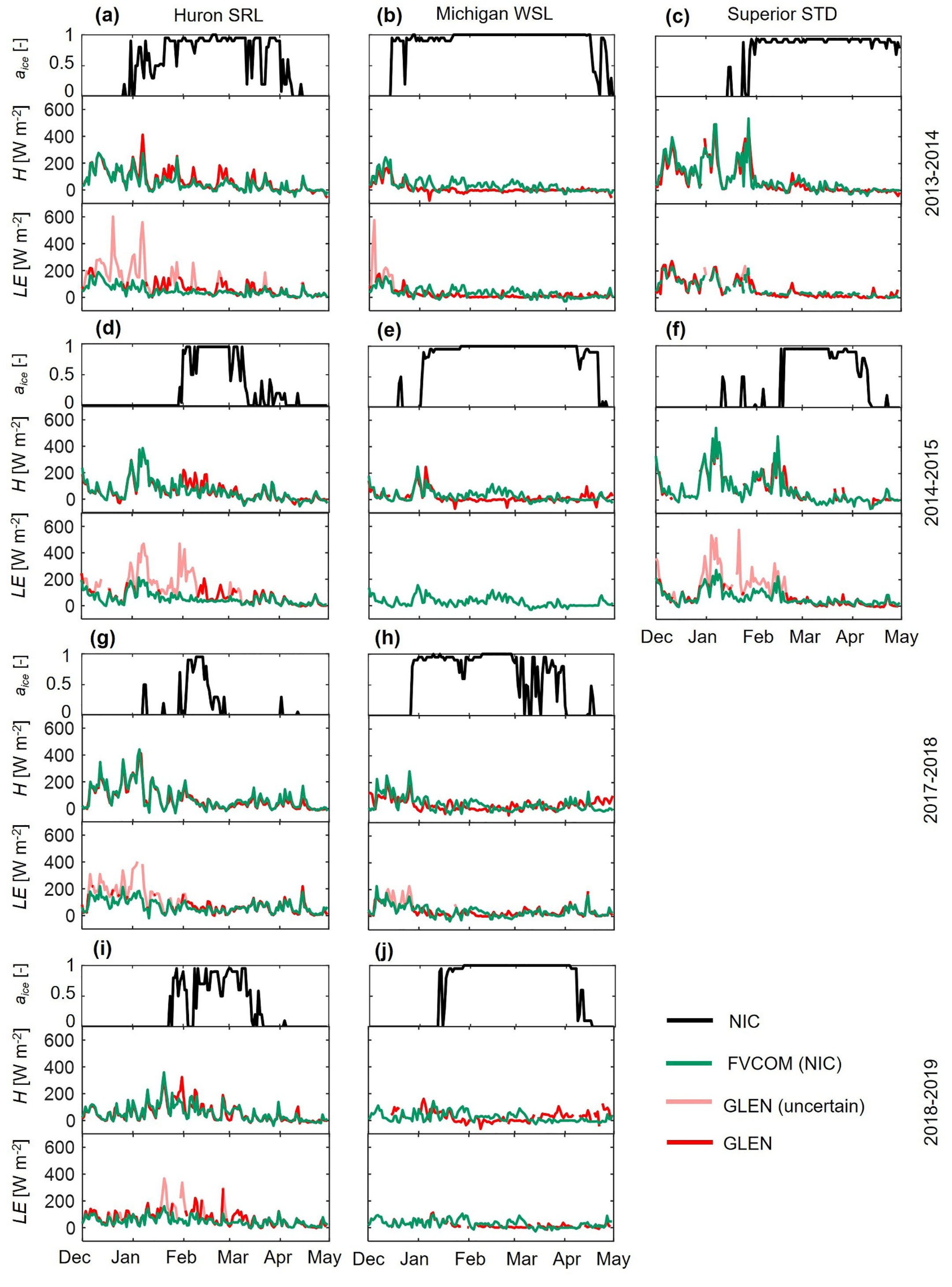

Figure 5. Time series of ice concentration from National Ice Center (black), sensible and latent heat fluxes with uncertain (light red), and filtered Great Lakes Evaporation Network (red) data and Finite Volume Community Ocean Model (green) at (a, d, g, i) Spectacle Reef, (b, e, h, j) White Shoal, and (c, f) Stannard Rock stations for (a–c) 2013–2014, (d–f) 2014–2015, (g, h) 2017–2018, and (i, j) 2018–2019 winters.

We evaluated the model using daily turbulent heat flux RMSEs summarized in Table 2 for each lake and winter. We also show latent heat flux RMSEs with the uncertain data included and filtered out. For all lakes and winters, the mean RMSEs were ∼40 W m^{-2} and ∼30 W m^{-2} for sensible and latent heat flux, respectively. There is some

Table 2
Summary Table of the Sensible and Latent Heat Flux RMSEs With the Finite Volume Community Ocean Model Model and Great Lakes Evaporation Network (GLEN) Data, With (in Parentheses) and Without the Uncertain GLEN Data for the Latent Heat Flux

	Huron SRL		Michigan WSL		Superior STD		All sites	
Flux RMSE [W m^{-2}]	*H*	*LE*	*H*	*LE*	*H*	*LE*	*H*	*LE*
2013–2014	37.6	(97.5) 37.0	43.2	(58.5) 33.1	45.0	(26.4) 21.6	41.9	(60.8) 30.6
2014–2015	30.3	(95.4) 35.6	38.9	–	44.2	(87.4) 22.0	37.8	(91.4) 28.8
2017–2018	24.8	(61.7) 22.2	49.7	(30.9) 25.4	–	–	37.3	(46.3) 23.8
2018–2019	33.9	(58.4) 39.1	55.4	(27.1) 27.2	–	–	44.7	(44.8) 33.2
All winters	31.7	(78.3) 33.5	46.8	(38.8) 28.6	44.6	(56.9) 21.8	40.3	(60.4) 29.2

variability between different years, but RMSEs vary between 38 and 45 W m^{-2} for *H* and between 24 and 33 for *LE*. There is even more variability between stations, where RMSEs vary between 32 and 47 W m^{-2} for *H* and 22–34 W m^{-2} for *LE*. There are significantly smaller sensible heat flux errors at Lake Huron's SRL station than at the other two stations, which also have the highest latent heat flux errors. When the uncertain *LE* data are included, it results in greater variation in the RMSEs (shown in parentheses in Table 2). While there are periods without much difference compared to the filtered RMSEs, in most cases, RMSEs increase two to four times higher and reach almost 100 W m^{-2} using the raw GLEN latent heat flux data.

Based on all simulations, we compare modeled and observed fluxes in Figure 6. The gray color shows the uncertain GLEN data. In Figures 6a and 6b, we show the original FVCOM fluxes fractioned by the FVCOM ice concentrations for the whole season, colored by the NIC ice concentrations. We see high NIC ice concentrations and very low fluxes; the RMSE for sensible and latent heat flux is 53.6 and 34.7 W m^{-2}, respectively. In Figures 6c and 6d, we show NIC fractioned fluxes for the whole seasons colored by ice concentration bias (modeled minus observed), where we see reduced RMSEs, which are 40.7 and 30.0 W m^{-2} for sensible and latent heat flux, respectively. Despite the ice error (the NIC corrected), modeled fluxes agree with the observations. In Figures 6e and 6f, we only show fluxes for open water conditions when NIC ice concentrations are below 0.1, colored by temperature differences. The model fluxes are even better, resulting in RMSEs of 36.5 and 24.4 W m^{-2} for *H* and *LE*, respectively. The model shows a small overestimation for the high sensible heat fluxes. In Figures 6g and 6h, we only show fluxes for nearly complete ice-covered conditions when NIC ice concentrations are above 0.9, colored by the NIC ice thickness. Here, we find a worse match between the model and observations, resulting in RMSEs of 45.4 and 35.0 W m^{-2} for *H* and *LE*, respectively. Here, both sensible and latent heat fluxes have similarly high errors. When the thickness is low (blue dots), the model can either underestimate or overestimate the fluxes. Sometimes, in the case of high thickness (red dots) the model underestimates the fluxes, likely due to the residual error in the modeled ice thickness, surface temperatures, and ice fluxes (even when concentration is adjusted to the NIC). In contrast, when the thickness is medium-high (yellow dots), the model fluxes are too high compared to the GLEN data.. This suggests that the ice thickness strongly influences ice fluxes, while currently, the air-ice flux calculation method does not consider ice thickness.

To further analyze this problem, we show the FVCOM modeled and GLEN observed sensible heat fluxes by stations, separately for freezing (Figures 7a–7i) and melting (Figures 7j–7r) as well. Periods were selected manually for each simulation based on the NIC data. Each row shows the same data points but colored differently by NIC ice concentrations (Figures 7a–7c and 7j–7l), ice surface and air temperature differences (Figures 7d–7f and 7m–7o), and NIC ice thicknesses (Figures 7g–7i and 7p–7r). There is no data for STD for melting because it extended beyond the simulation period. The results clearly show by the ice concentration coloring that there is limited fractional ice data in the NIC, as most values are near-zero or 100% ice. At the same time, flux values are generally well modeled for lower ice concentrations, but larger deviations occur when high ice concentrations occur. This could be due to erroneous ice fluxes, but may be more likely caused by NIC's overestimation of ice concentrations and failure to resolve subgrid-scale fractures. In general, the ice surface and air temperature differences, as well as the flux values, are higher in the freezing period, and while the NIC ice thickness is only a rough approximation, there is lower ice thickness in the freezing period. When melting at WSL, there are many flux errors

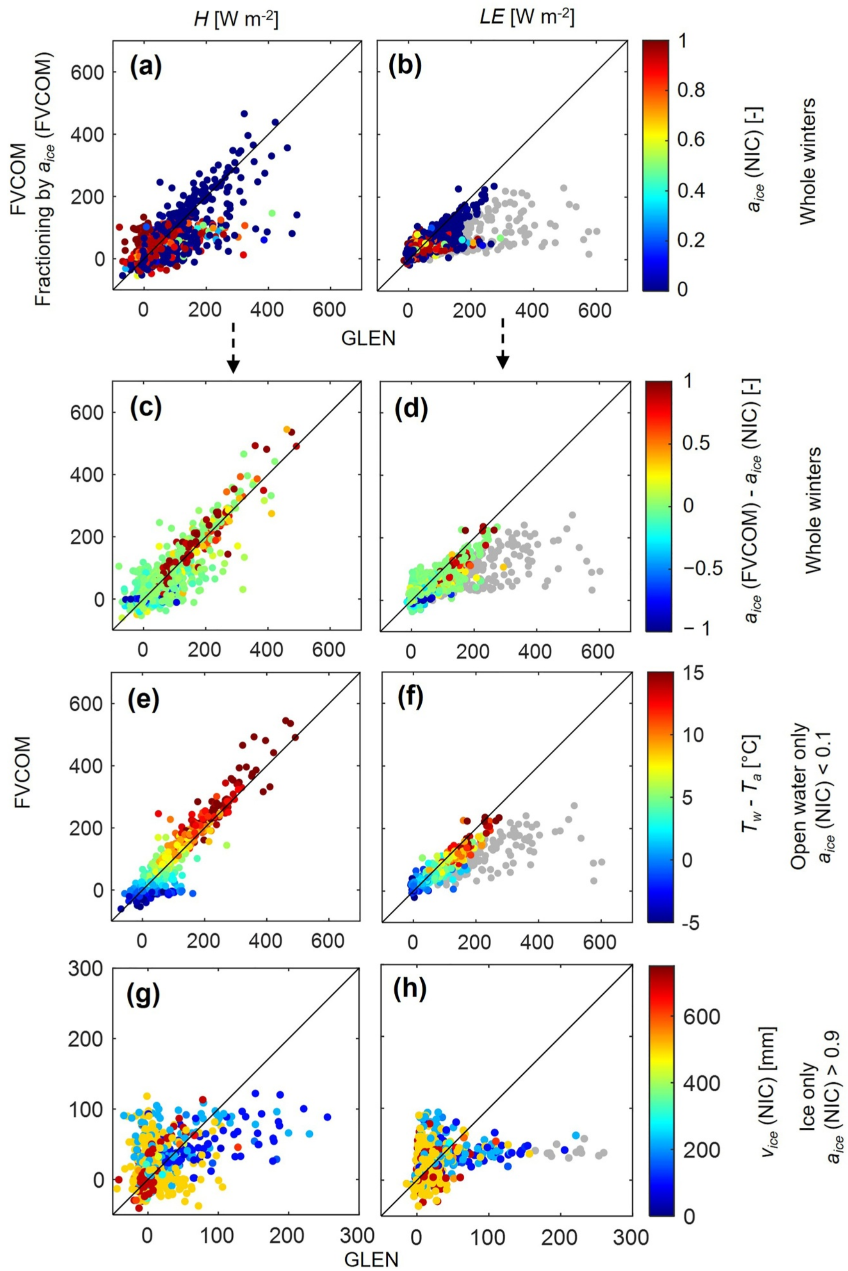

Figure 6. Finite Volume Community Ocean Model (FVCOM) modeled, and Great Lakes Evaporation Network (GLEN) observed (a, c, e, g) sensible and (b, d, f, h) latent heat fluxes for (a)–(b) whole winters colored by National Ice Center (NIC) ice concentrations with FVCOM ice fractioning, (c)–(d) whole winters colored by ice concentration bias (modeled minus observed), (e)–(f) open water only colored by the lake-air temperature differences, (g)–(h) ice cover colored by NIC ice. Uncertain GLEN flux data are shown in gray. For (c–h) we use NIC ice fractioning of fluxes similar to other figures.

related to low temperature differences and thick ice compared to the GLEN data. Although not shown, the latent heat fluxes demonstrate similar patterns.

For complete or nearly-complete ice cover, we show modeled and observed sensible and latent fluxes by each station, including a simple fractioning modification using the model data (Figure 8). Data are colored by the ice surface and air temperature differences (Figures 8a–8f) and the mean of the NIC-estimated ice thickness intervals (Figures 8g–8r). There are smaller flux errors in the case of the sensible heat flux, which may be related to the GLEN latent heat flux uncertainties. There are significant differences between the flux error, temperature

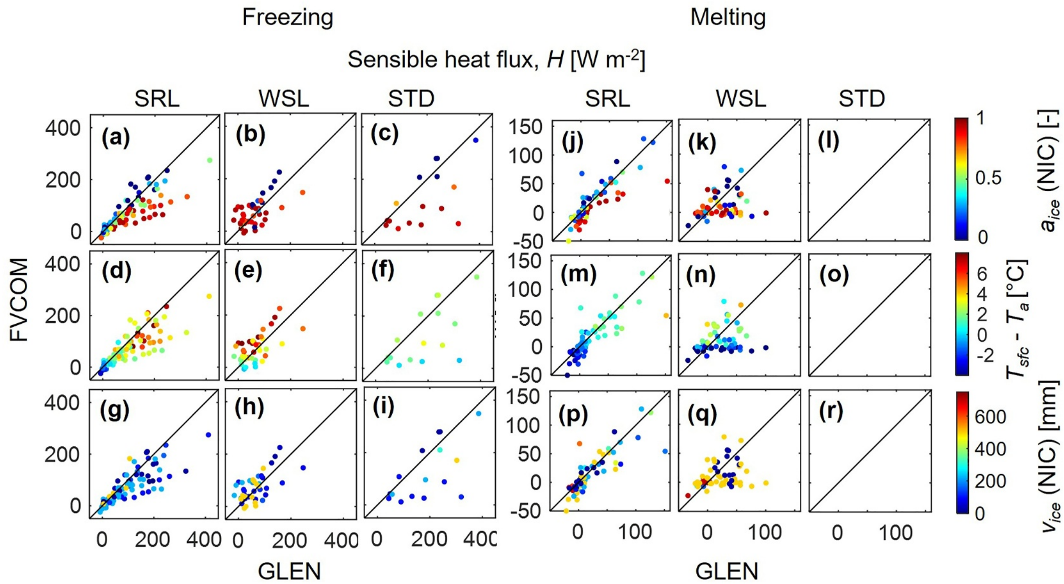

Figure 7. Finite Volume Community Ocean Model modeled and Great Lakes Evaporation Network observed sensible heat fluxes for (a–i) freezing and (j–r) melting periods for each station for fractional ice. Colored by (a–c, j–l) National Ice Center (NIC) ice concentration, (d–f, m–o) modeled ice surface and air temperature difference, and (g–i, p–r) NIC ice thickness.

difference, and ice thickness for each station. Again, the NIC ice thickness has some uncertainty since it is only a rough estimation; however, we found notable relationships. Even though the number of data points are limited, the model underestimations seem larger in the case of thin ice for higher *H* and *LE* fluxes. When STD experiences thick ice of 700 mm, the FVCOM flux estimation improves. WSL station has thick ice of 500 mm for most simulation periods, and the GLEN observed sensible and latent heat fluxes are very low. The near-zero fluxes could also be site-specific for WSL, which is shallower, and waves and ice movement are limited due to the Straits of Mackinac at the connection between Lakes Michigan and Huron, where ice can build up without cracks.

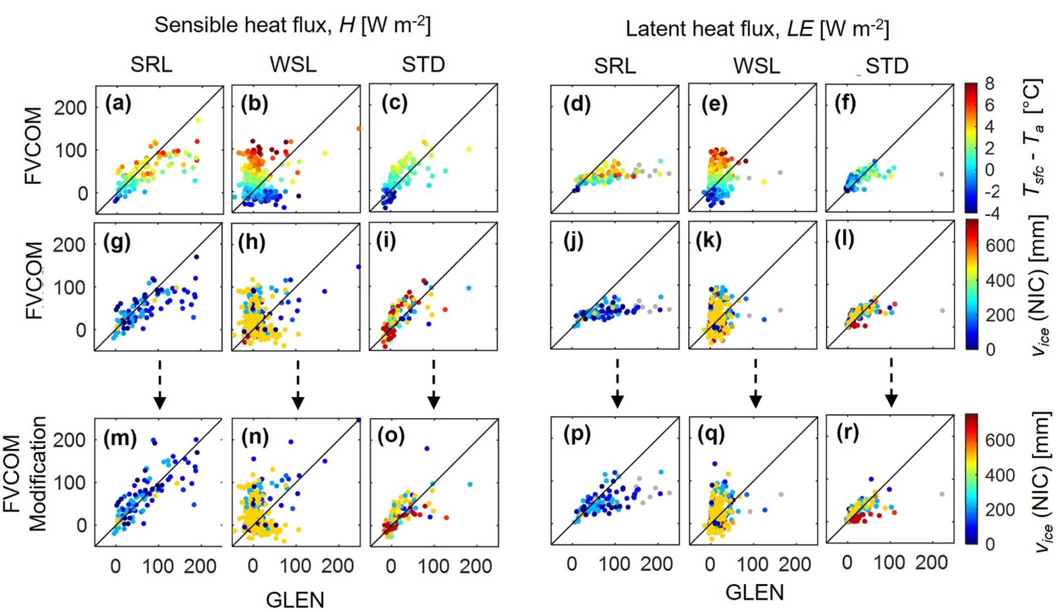

Figure 8. Finite Volume Community Ocean Model modeled and Great Lakes Evaporation Network observed (a–c, g–i, m–o) sensible and (d–f, j–l, p–r) latent heat fluxes for each station for near-full ice cover only, where (m–r) show modified flux fractioning based on ice thickness. Colored by (a–c, d–f) ice surface and air temperature difference, and (g–r) National Ice Center ice thickness.

We note that our study aimed to analyze fluxes during periods of partial ice concentrations, aside from the separate open water and fully ice-covered conditions. However, both the NIC data and modeled ice concentrations reveal very few periods of partial ice at the stations where flux data is available, whether that is realistic or not. Due to its spatial and temporal resolution, the NIC data is unlikely to represent the true dynamic ice field, and yet the CICE continuum ice model is also limited in its ability to resolve finer-scale features. This can lead to errors in both the ice and the flux predictions that should be considered in model validation.

4. Discussion

4.1. Potential Model Improvement

We suggest adjustments be made in addition to pro-rating flux by ice concentration in the future, as it is not the only contributing factor. An example would be changing the fractioning equation for different ice thickness ranges. We test a simple calculation using the FVCOM-CICE and COARE fluxes and modifying the ratio of the open water fluxes (Figures 8m–8r) for the very thin ice below 100 mm and thick ice above 500 mm. There is some visible improvement at SRL, and some of the high fluxes are reduced at WSL too; however, there are a couple of points where fluxes became even less accurate compared to the GLEN. We do not calculate RMSE improvement because these flux changes interact with the other hydrodynamic and ice processes that should be considered. Different model modifications based on ice thickness (or other variables) should be tested in the FVCOM model and compared with flux and ice data to improve the operation forecasts in the future.

4.2. Comparison With Other Studies

Charusombat et al. (2018) carried out a detailed flux analysis of the Great Lakes, testing several flux models for the ice-free periods between 2012 and 2014. Fluxes were evaluated against GLEN data for the same three stations as in our study and one additional location. COARE performed the best out of the models, and they revised the parameterization of the other models to improve their respective model fluxes. Similar to our findings, they obtained low RMSEs for the sensible heat flux for all three stations. The latent heat flux RMSE was similarly low for STD and WSL, while SRL yielded higher values. Interestingly, while the revised parameterizations improved sensible heat fluxes at all three stations, the same degree was not reflected in latent heat fluxes at STD and WSL, and model skill even deteriorated at SRL. Xue et al. (2024) also did a detailed evaluation of coupled lake-ice-atmosphere models, including assessing modeled and measured turbulent heat fluxes. Their analysis covered the winter of 2014–2015, as in our study, and their 3D lake model simulations resulted in a good match with the GLEN data for sensible heat fluxes but showed high errors for latent heat fluxes at SRL. At the same time, both modeled fluxes were in good agreement with the measured ones at another station, Granite Island in Lake Superior. At the beginning of January 2015, the daily GLEN latent heat fluxes highly differ at these two stations, with ~200 W m^{-2} at Granite Island and ~400 W m^{-2} at SRL on average, while the coupled model system simulated similar, ~200 W m^{-2} values at both locations. We note that Granite Island was using an LI-7500 that year, and SRL was using a KH20 krypton hygrometer. In short, the study of Charusombat et al. (2018) confirms that the employed COARE algorithm can be a reliable choice for flux calculations, while the similar results of Xue et al. (2024) suggest the potential for uncertainty in the measured data in our analysis, which will be discussed further.

4.3. Flux Uncertainties

In the results, we showed two evaluations, one with the full data set and one excluding some high latent fluxes. In the following section, we corroborate why specific periods of observed latent heat fluxes might be best disregarded in the evaluation of the FVCOM model, as these measured values are inexplicably high.

Figure 9 shows daily latent heat fluxes from STD against the product of wind speed and specific humidity gradients for both winters (between December 1st and February 1st). Water surface temperatures were taken from the GLSEA data. Data points follow a nearly linear regression line with a small scatter for both 2013–2014 and 2014–2015. There are a few outliers during 2013–2014 with low latent heat flux values, which may have been caused by the lake ice at the end of January 2014 (ice is not accounted for in the specific humidity gradient). However, these values were also captured by the model, as shown in Figure 4. However, the high-value outliers of January 2015 (shown in yellow) deviate significantly from the quasilinear relationship in Figure 9. If we consider

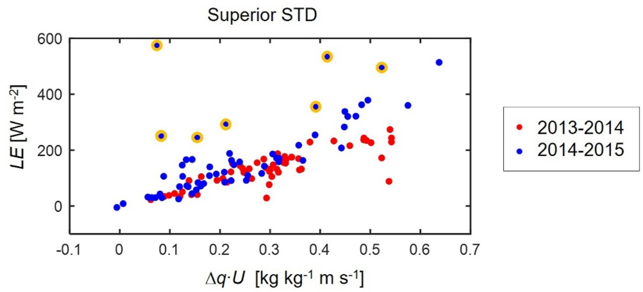

Figure 9. Daily latent heat fluxes as a function of the product of wind speed and specific humidity gradients at Lake Superior's Stannard Rock station between December 1st and February 1st in winter 2013–2014 (red), 2014–2015 (blue), and uncertain values are shown with yellow circles.

these outliers to be unrealistically high, then we could define a bulk threshold above which daily latent heat fluxes should be considered cautiously.

To resolve the suspicion of unrealistically high latent heat fluxes, we performed a simple but robust sensitivity analysis. We reran the COARE model assuming ice-free, open-water periods by perturbing the forcing data (wind speed, air temperature, and relative humidity) to obtain a maximum possible upper limit and, thus, a metric for realistic flux values. We used the original time series with modifications of (a) increasing wind speed by 20%, (b) increasing air-water temperature difference by +5°C (to intensify atmospheric instability), and (c) decreasing relative humidity by 20% (to increase the vertical humidity gradient). We analyzed these modifications separately, but their combined application resulted in the largest fluxes; thus, we only show those. Figure 10 shows a daily time series of ice concentrations, sensible, and latent heat fluxes with the original COARE and with perturbed forcings as a realistic upper limit for the two winters for STD. As a result of the modifications, sensible heat fluxes are significantly overestimated for both winters, mainly caused by the increased air-water temperature difference. The 20% increase in wind speed alone did not significantly change either of the two heat fluxes, as the fluxes are highly affected by atmospheric stability during highly unstable conditions in winter. In the case of latent heat flux, the differences are not significant, but it is clearly notable that the very high *LE* values cannot be reached with the COARE-based upper limit estimates, even when completely ice-free conditions were imposed.

Figure 11 shows the *LE* bias, air temperature, and daily precipitation time series for winter 2014–2015 at the STD station. Inspection of these time series reveals that it is possible that the latent heat flux measurements were affected by frozen droplets on the EC instrumentation (Campbell Scientific KH20 krypton hydrometer), as precipitation events and very low temperatures preceded and accompanied the days with *LE* high bias. Moreover, in several periods, the *LE* bias increased and decreased in parallel with the air temperature. Frozen precipitation could include various types, including frost, freezing rain, fog, spray, and snow, and we suspect that frost and freezing fog or spray could impact errors more than snow. In short, extreme meteorological conditions can result in measurement inaccuracy, which could explain the anomalous values, but further sensor information would be needed to confirm this hypothesis.

Nicholls et al. (2024) published the Stannard Rock flux data in the AmeriFlux data archive. STD had two gas analyzers operating simultaneously from 2008 until 2022 with occasional gaps. We compared daily latent heat

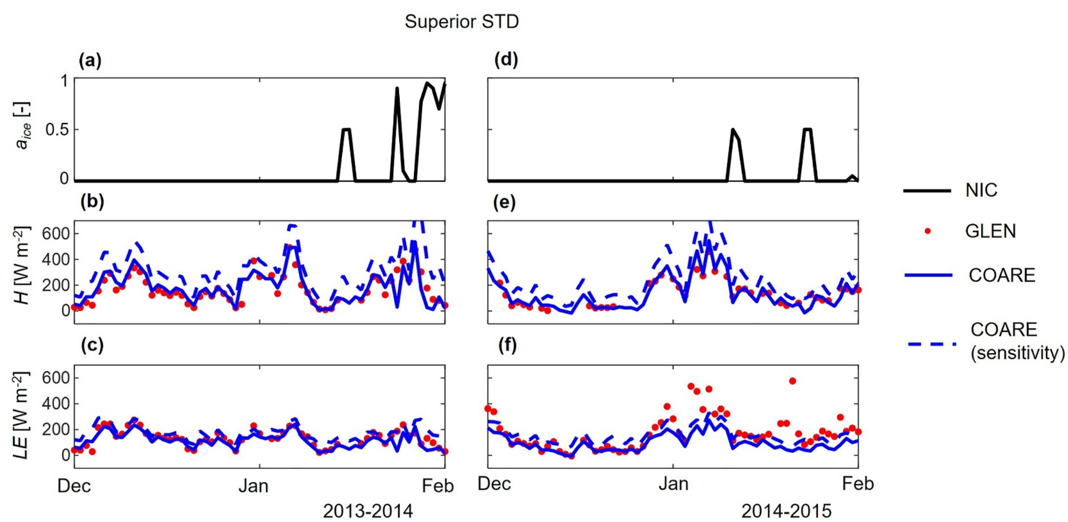

Figure 10. Time series of (a), (d) National Ice Center ice concentrations, (b), (e) sensible and (c), (f) latent heat fluxes at Lake Superior's Stannard Rock station in winter (a)–(c) 2013–2014 and (d)–(f) 2014–2015 with Great Lakes Evaporation Network data (red), Coupled Ocean-Atmosphere Response Experiment (COARE) (blue), and COARE sensitivity analysis (dashed blue).

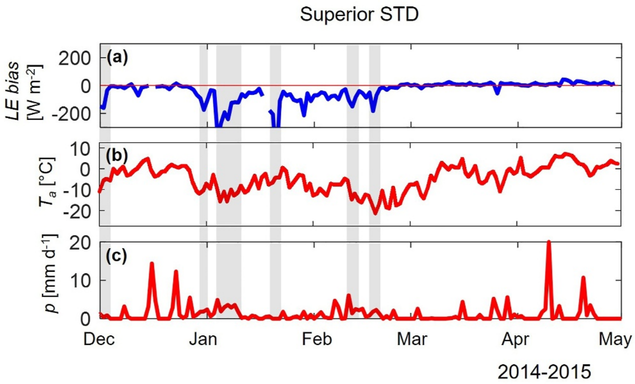

Figure 11. Time series of (a) latent heat flux bias (model minus observed), (b) observed interpolated air temperature, and (c) model precipitation at Lake Superior's Stannard Rock station in winter 2014–2015. Precipitation, cold air temperatures, and high latent heat flux are highlighted in gray.

fluxes in winter and plotted the two instruments' fluxes against each other (Figure 12). The KH20 krypton hydrometer consistently measured higher flux values than the LI-7500 IRGA instrument by roughly 25%–30%, even though Nicholls et al. (2024) used a stricter quality control than the GLEN. This agrees with our findings that most stations and years with KH20 had unrealistically high *LE* values during winter, while the LI-7500 measured values in 2013–2014 at STD matched the modeled fluxes. The differences between the two instruments are much smaller in the summer period (Nicholls et al., 2024).

In summary, in the case of STD, based on the $\Delta q \cdot U$ and *LE* relationships, we believe it is reasonable to exclude those values and periods from the model evaluation. Therefore, for the model evaluation, we calculated the errors using filtered data sets since the sensitivity analysis-based upper limits confirmed our suspicion.

4.4. Meteorology Forcing

The quality of the meteorology input may highly influence the output of the hydrodynamic model. In this study, we have used interpolated meteorology forcing based on the available stations around the lake and the GLEN stations located in the open water, a common approach in Great Lakes modeling for years that extends before the availability of modern forecast products such as the NOAA High-Resolution Rapid Refresh (HRRR; Benjamin et al., 2016). Figure 13 shows the turbulent flux time series with and without including Spectacle Reef station data in the interpolation for the meteorology forcing of the model. With Spectacle Reef included, the FVCOM model estimates match significantly better with the GLEN data in the case of sensible heat flux. Regarding latent heat fluxes, the impact of including open water stations is less pronounced but still noticeable. We found that the effect of including an open water station can be high, especially at the beginning of winter. The smaller deviations in the middle of the winter are most likely due to ice errors in the NIC for sensible heat. In the case of latent heat, both ice errors and the observed flux uncertainties described earlier are present. It is not surprising that the meteorological forcing is crucial to the model's accuracy, but it underscores the importance of open water observations and data assimilation into weather forecast products.

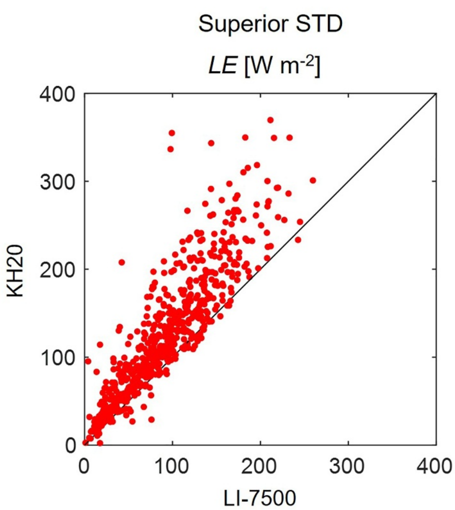

Figure 12. Daily latent heat fluxes at Superior's Stannard Rock station during winter from December 1st until March 1st between 2008 and 2022 from the AmeriFlux database with two instruments (LI-7500 IRGA and KH20 krypton hygrometer gas analyzers).

5. Conclusion

In this study, we evaluated winter turbulent heat exchanges modeled by the coupled hydrodynamic-ice model (FVCOM-CICE) of the Great Lakes used for operational forecasts. Hindcast simulations were made for several winter periods driven by interpolated meteorological forcing based on the available station data around the lakes. We analyzed model outputs, that is, surface temperature, ice condition, and turbulent heat fluxes for three lakes for ice-free, ice-covered, and partial ice conditions. We assessed the modeled fluxes with EC observations from the GLEN.

In the case of the Great Lakes, turbulent heat fluxes peak in the fall and early winter due to large temperature gradients and high wind speeds. The model accurately captured the open water fluxes. With the appearance of ice, differences in the measured and modeled turbulent fluxes were observed, due to several factors. On the one hand, FVCOM ice output errors can result in a heat flux bias due to a misleading ice concentration. On the other hand, modeled heat fluxes cannot be adequately assessed due to the lack of ice surface temperature data. Finally, we found a convincing relationship between flux errors and ice thickness based on the flux observations. However, ice thickness data from the National Ice Center is not derived from direct measurement; therefore, its accuracy is unknown. Thin, melting ice has many small cracks and water on top of the ice that may result in nearly as high fluxes as open water conditions. In contrast, very thick ice may reduce heat fluxes to

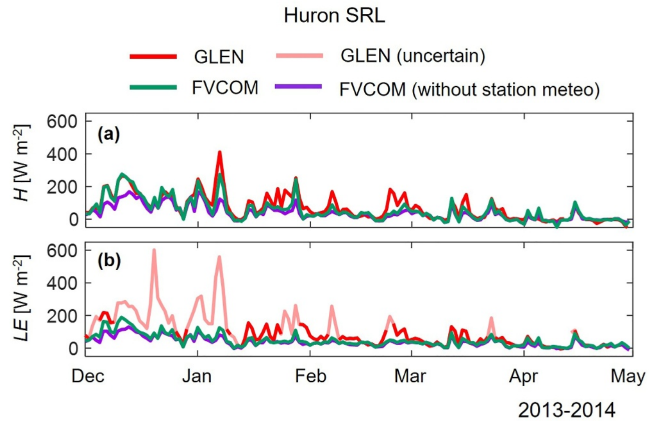

Figure 13. Time series of (a) sensible and (b) latent heat fluxes at Lake Huron's Spectacle Reef station in winter 2013–2014 with Finite Volume Community Ocean Model (FVCOM) using open water station meteorology in the forcing (green), with FVCOM without open water station data in the forcing (purple), and with Great Lakes Evaporation Network data (red), uncertain values shown with light red.

near zero, from which one can assume that ice surface temperature is closely equal to air temperature in these cases. In the future, including ice thickness in the model's flux calculation could improve temperature and ice forecasts. The model development is especially important because of the declining ice concentration and the more partial and thinner ice due to climate change. Finally, we found anomalous observed latent heat fluxes with unrealistically high values both during ice-free and ice-covered periods, especially during freezing in early winter with low temperatures and frozen precipitation. These observational data during such conditions should be used cautiously for model validations.

Conflict of Interest

The authors declare no conflicts of interest relevant to this study.

Data Availability Statement

All data used in this study are publicly available. The flux observation data from the GLEN is openly available from NOAA GLERL (2023a) using huron-srl, mish-wsl, and superior-std folders for the SRL, WSL, and STD stations, respectively, using different folders for years, and using sensor_format and ec_data folders to reach the data. STD flux data is available on AmeriFlux (Nicholls et al., 2024). The FVCOM-CICE model v4.4 is openly available on GitHub (Chen, 2023; Chen et al., 2003), and the NOAA-GLOFS configuration is available from NOAA GLERL (2023c) for Lake Superior (LSOFS) and Michigan-Huron (LMHOFS). Surface temperature data used are available from NOAA GLERL (2023d). Great Lakes ice data are available from the U.S. National Ice Center (2023). Meteorological data used for the simulations are available from NOAA GLERL (2023b) by clicking on the station and viewing all data.

Acknowledgments
We highly appreciate the contributions of David M. Wright and Lauren M. Fry to this research. The research presented in the article was carried out within the framework of the Széchenyi Plan Plus program with the support of the RRF 2.3.121202200008 project, and by the Sustainable Development and Technologies National Program of the Hungarian Academy of Sciences (FFT NP FTA). Peter Torma was funded by the Hungarian Academy of Sciences (Janos Bolyai Fellowship, 00906/23).

References

Anderson, E. J., Fujisaki-Manome, A., Kessler, J., Lang, G. A., Chu, P. Y., Kelley, J. G. W., et al. (2018). Ice forecasting in the next-generation Great Lakes Operational Forecast System (GLOFS). *Journal of Marine Science and Engineering*, *6*(4), 123. https://doi.org/10.3390/jmse6040123

Anderson, E. J., Tillotson, B., & Stow, C. A. (2024). Indications of a changing winter through the lens of lake mixing in Earth's largest freshwater system. *Environmental Research Letters*, *19*(12), 124060. https://doi.org/10.1088/1748-9326/ad8ee0

Assel, R. A. (2005). Classification of annual Great Lakes ice cycles: Winters of 1973-2002. *Journal of Climate*, *18*(22), 4895–4905. https://doi.org/10.1175/JCLI3571.1

Benjamin, S. G., Weygandt, S. S., Brown, J. M., Hu, M., Alexander, C. R., Smirnova, T. G., et al. (2016). A North American hourly assimilation and model forecast cycle: The rapid refresh. *Monthly Weather Review*, *144*(4), 1669–1694. https://doi.org/10.1175/mwr-d-15-0242.1

Blanken, P. D., Spence, C., Hedstrom, N., & Lenters, J. D. (2011). Evaporation from Lake Superior: 1. Physical controls and processes. *Journal of Great Lakes Research*, *37*(4), 707–716. https://doi.org/10.1016/j.jglr.2011.08.009

Cannon, D., Wang, J., Fujisaki-Manome, A., Kessler, J., Ruberg, S., & Constant, S. (2024). Investigating multidecadal trends in ice cover and subsurface temperatures in the laurentian Great Lakes using a coupled hydrodynamic-ice model. *Journal of Climate*, *37*(4), 1249–1276. https://doi.org/10.1175/JCLI-D-23-0092.1

Charusombat, U., Fujisaki-Manome, A., Gronewold, A. D., Lofgren, B. M., Anderson, E. J., Blanken, P. D., et al. (2018). Evaluating and improving modeled turbulent heat fluxes across the North American Great Lakes. *Hydrology and Earth System Sciences*, *22*(10), 5559–5578. https://doi.org/10.5194/hess-22-5559-2018

Chen, C. (2023). Finite Volume Community Ocean Model (FVCOM) version 4.4 [Software]. *GitHub*. https://github.com/FVCOM-GitHub/FVCOM/

Chen, C., Liu, H., & Beardsley, R. C. (2003). An unstructured grid, finite-volume, three-dimensional, primitive equations ocean model: Application to coastal ocean and estuaries [Software]. *Journal of Atmospheric and Oceanic Technology*, *20*(1), 159–186. https://doi.org/10.1175/1520-0426(2003)020<0159:AUGFVT>2.0.CO;2

Croley, T. E. (1989). Lumped modeling of Laurentian Great Lakes evaporation, heat storage, and energy fluxes for forecasting and simulation NOAA Technical Memorandum ERL GLERL-70. https://repository.library.noaa.gov/view/noaa/11262/noaa_11262_DS1.pdf

Culpepper, J., Sharma, S., Gunn, G., Magee, M. R., Meyer, M. F., Anderson, E. J., et al. (2025). One-hundred fundamental, open questions to integrate methodological approaches in lake ice research. *Water Resources Research*, *61*(5), e2024WR039042. https://doi.org/10.1029/2024WR039042

Durnford, D., Fortin, V., Smith, G. C., Archambault, B., Deacu, D., Dupont, F., et al. (2018). Toward an operational water cycle prediction system for the Great Lakes and St. Lawrence River. *Bulletin of the American Meteorological Society*, *99*(3), 521–546. https://doi.org/10.1175/bams-d-16-0155.1

Frank, J. M., & Massman, W. J. (2023). A study of the role of seven historically significant fast-response hygrometers and sensor calibration on eddy covariance H_2O fluxes and surface energy balance closure. *Agricultural and Forest Meteorology*, *334*, 109437. https://doi.org/10.1016/j.agrformet.2023.109437

Fairall, C. W., Bradley, E. F., Hare, J. E., Grachev, A. A., & Edson, J. B. (2003). Bulk parameterization of air–sea fluxes: Updates and verification for the COARE algorithm. *Journal of Climate*, *16*(4), 571–591. https://doi.org/10.1175/1520-0442(2003)016<0571:bpoasf>2.0.co;2

Fry, L. M., Gronewold, A. D., Seglenieks, F., Minallah, S., Apps, D., & Ferguson, J. (2022). Navigating Great Lakes hydroclimate data. *Frontiers in Water*, *4*, 803869. https://doi.org/10.3389/frwa.2022.803869

Fujisaki-Manome, A., Anderson, E. J., Kessler, J. A., Chu, P. Y., Wang, J., & Gronewold, A. D. (2020). Simulating impacts of precipitation on ice cover and surface water temperature across large lakes. *Journal of Geophysical Research: Oceans*, *125*(5), e2019JC015950. https://doi.org/10.1029/2019jc015950

Fujisaki-Manome, A., Fitzpatrick, L. E., Gronewold, A. D., Anderson, E. J., Lofgren, B. M., Spence, C., et al. (2017). Turbulent heat fluxes during an extreme lake-effect snow event. *Journal of Hydrometeorology*, *18*(12), 3145–3163. https://doi.org/10.1175/JHM-D-17-0062.1

Fujisaki-Manome, A., Mann, G. E., Anderson, E. J., Chu, P. Y., Fitzpatrick, L. E., Benjamin, S. G., et al. (2020). Improvements to lake-effect snow forecasts using a one-way air–lake model coupling approach. *Journal of Hydrometeorology*, *21*(12), 2813–2828. https://doi.org/10.1175/JHM-D-20-0079.1

Gronewold, A. D., Anderson, E. J., Lofgren, B., Blanken, P. D., Wang, J., Smith, J., et al. (2015). Impacts of extreme 2013-2014 winter conditions on Lake Michigan's fall heat content, surface temperature, and evaporation. *Geophysical Research Letters*, *42*(9), 3364–3370. https://doi.org/10.1002/2015GL063799

Gronewold, A. D., Fortin, V., Caldwell, R., & Noel, J. (2018). Resolving hydrometeorological data discontinuities along an international border. *Bulletin of the American Meteorological Society*, *99*(5), 899–910. https://doi.org/10.1175/BAMS-D-16-0060.1

Guseva, S., Armani, F., Desai, A. R., Dias, N. L., Friborg, T., Iwata, H., et al. (2023). Bulk transfer coefficients estimated from eddy-covariance measurements over Lakes and reservoirs. *Journal of Geophysical Research: Atmospheres*, *128*(2), e2022JD037219. https://doi.org/10.1029/2022JD037219

Hunke, E., Lipscomb, W., Jones, P., Turner, A., Jeffery, N., & Elliott, S. (2017). *CICE, the Los Alamos sea ice model (No. CICE; 005315WKSTN00)*. Los Alamos National Laboratory (LANL).

Lenters, J. D., Anderton, J. B., Blanken, P., Spence, C., & Suyker, A. E. (2013). Assessing the impacts of Climate Variability and Change on Great Lakes Evaporation: Implications for water levels and the need for a coordinated observation network. *Great Lakes Evaporation: Implications for Water Levels*, *11*. http://glisaclimate.org/media/GLISA_Lake_Evaporation.pdf

Lin, Y., Fujisaki-Manome, A., & Anderson, E. J. (2022). Simulating landfast ice in Lake Superior. *Journal of Marine Science and Engineering*, *10*(7), 932. https://doi.org/10.3390/jmse10070932

Liu, P. C., & Schwab, D. J. (1987). A comparison of methods for estimating u* from given u_z and air-sea temperature differences. *Journal of Geophysical Research*, *92*(C6), 6488–6494. https://doi.org/10.1029/JC092iC06p06488

Lükő, G., Torma, P., Weidinger, T., & Krámer, T. (2022). Air-Lake momentum and heat exchange in very young waves using energy and water budget closure. *Journal of Geophysical Research: Atmospheres*, *127*(12), e2021JD036099. https://doi.org/10.1029/2021JD036099

Nicholls, E. M., Spence, C., Hedstrom, N., Lenters, J. D., & Blanken, P. D. (2024). Lake Superior evaporation: A long-term eddy covariance dataset at Stannard Rock Lighthouse (2008-2022) [Dataset]. *Scientific Data*, *11*(1). https://doi.org/10.1038/s41597-024-03940-7.1152.

NOAA GLERL. (2023a). Eddy covariance measured turbulent heat flux data for the Great Lakes [Dataset]. Retrieved from https://www.glerl.noaa.gov/res/recon/data/bystation/

NOAA GLERL. (2023b). Great Lakes meteorological data [Dataset]. Retrieved from https://apps.glerl.noaa.gov/marobs/

NOAA GLERL. (2023c). Great Lakes Operational Forecast System model settings [Software]. Retrieved from https://www.ncei.noaa.gov/thredds/catalog/model/model.html

NOAA GLERL. (2023d). Great Lakes surface temperature data [Dataset]. Retrieved from https://coastwatch.glerl.noaa.gov/statistics/average-surface-water-temperature-glsea/

O'Reilly, C. M., Rowley, R. J., Schneider, P., Lenters, J. D., Mcintyre, P. B., & Kraemer, B. M. (2015). Rapid and highly variable warming of lake surface waters around the globe. Geophysical Research Letters, 42: 1-9. *Geophysical Research Letters*, 1–9. https://doi.org/10.1002/2015GL066235.Received

Phillips, W. D., & Irbe, J. G. (1978). Land-to-lake comparison of wind, temperature, and humidity on Lake Ontario during the international field year for the Great Lakes (IFYGL) rep. CLI-2-77. *Atmospheric Environment Service, Environment Canada, Downsview, Ontario*.

Resio, D. T., & Vincent, C. L. (1977). Estimation of winds over the Great Lakes. *Journal of the Waterway, Port, Coastal and Ocean Division*, *103*(2), 265–283. https://doi.org/10.1061/JWPCDX.0000027

Schwab, D. J., & Bedford, K. W. (1994). Initial implementation of the Great Lakes forecasting System: A real-time System for predicting Lake circulation and thermal structure. *Water Quality Research Journal*, *29*(2–3), 203–220. https://doi.org/10.2166/wqrj.1994.014

Schwab, D. J., Leshkevich, G. A., & Muhr, G. C. (1999). Automated mapping of surface water temperature in the Great Lakes. *Journal of Great Lakes Research*, *25*(3), 468–481. https://doi.org/10.1016/S0380-1330(99)70755-0

Schwab, D. J., & Morton, J. A. (1984). Estimation of overlake wind speed from overland wind speed: A comparison of three methods. *Journal of Great Lakes Research*, *10*(1), 68–72. https://doi.org/10.1016/S0380-1330(84)71808-9

Sharma, A., Hamlet, A. F., Fernando, H. J. S., Catlett, C. E., Horton, D. E., Kotamarthi, V. R., et al. (2018). The need for an integrated land-lake-atmosphere modeling system, exemplified by North America's Great Lakes region. *Earth's Future*, *6*(10), 1366–1379. https://doi.org/10.1029/2018EF000870

Sharma, S., Blagrave, K., Magnuson, J. J., O'Reilly, C. M., Oliver, S., Batt, R. D., et al. (2019). Widespread loss of lake ice around the Northern Hemisphere in a warming world. *Nature Climate Change*, *9*(3), 227–231. https://doi.org/10.1038/s41558-018-0393-5

Spence, C., Blanken, P. D., Hedstrom, N., Fortin, V., & Wilson, H. (2011). Evaporation from Lake Superior: 2. Spatial distribution and variability. *Journal of Great Lakes Research*, *37*(4), 717–724. https://doi.org/10.1016/j.jglr.2011.08.013

U. S. National Ice Center. (2023). Great Lakes ice data [Dataset]. Retrieved from https://usicecenter.gov/Products/GreatLakesData

Williamson, C. E., Saros, J. E., Vincent, W. F., & Smol, J. P. (2009). Lakes and reservoirs as sentinels, integrators, and regulators of climate change. *Limnology & Oceanography*, *54*(6, part 2), 2273–2282. https://doi.org/10.4319/lo.2009.54.6_part_2.2273

Woolway, R. I. (2023). The pace of shifting seasons in lakes. *Nature Communications*, *14*(1), 1–10. https://doi.org/10.1038/s41467-023-37810-4

Woolway, R. I., Anderson, E. J., & Albergel, C. (2021). Rapidly expanding lake heatwaves under climate change. *Environmental Research Letters*, *16*(9), 094013. https://doi.org/10.1088/1748-9326/ac1a3a

Woolway, R. I., Huang, L., Sharma, S., Lee, S. S., Rodgers, K. B., & Timmermann, A. (2022). Lake ice will be less safe for recreation and transportation under future warming. *Earth's Future*, *10*(10), 1–15. https://doi.org/10.1029/2022EF002907

Woolway, R. I., Sharma, S., & Smol, J. P. (2022). Lakes in hot water: The impacts of a changing climate on aquatic ecosystems. *BioScience*, *72*(11), 1050–1061. https://doi.org/10.1093/biosci/biac052

Xue, P., Huang, C., Zhong, Y., Notaro, M., Kayastha, M. B., Zhou, X., et al. (2024). Enhancing Winter climate simulations of the Great Lakes: Insights from a new coupled lake-ice-atmosphere (CLIAv1) model on the importance of integrating 3D hydrodynamics with a regional climate model. *Geoscientific Model Development*. https://doi.org/10.5194/gmd-2024-146

Yeo, A. J., Anderson, E. J., Jablonowski, C., Wright, D. M., Mann, G. E., Fujisaki-Manome, A., et al. (2024). Assessing the potential for medium-range ice forecasts in the laurentian Great Lakes. *Water Resources Research*, *60*(9), e2024WR037507. https://doi.org/10.1029/2024WR037507